

MODELLING OF SOLAR DISTILLATION SYSTEM WITH PHASE CHANGE MATERIAL STORAGE MEDIUM

by

Ali A. F. AL-HAMADANI and Shailendra K. SHUKLA*

Department of Mechanical Engineering, Indian Institute of Technology, Banaras Hindu University,
Varanasi, India

Original scientific paper
DOI: 10.2298/TSCI120102110A

An experimental investigation on a passive solar still with myristic acid as phase change material is carried out to examine the effect of both the mass of phase change material and basin water on the daily distillate output and efficiency of the system under indoor simulated condition. Basic energy balance equations are written to predict the water and glass temperatures, daily distillate output and instantaneous efficiency of the single slope solar distillation system with phase change material. It is found that the higher mass of phase change material with lower mass of water in the solar still basin significantly increases the daily yield and efficiency, but when the amount of phase change material exceeds 20 kg productivity reduces. Therefore, a novel and simple of solar stills with phase change material is proposed to enhance the overall productivity of the distillation system. The new solar still has increased the distillate output by 35-40%. The use of inner glass cover temperature for productivity prediction has also been investigated, and the prediction shows relatively better agreement with the experimental data.

Keywords: solar stills, phase change material, productivity,
heat transfer coefficients

Introduction

The importance of supplying hygienic clean and potable water can hardly be overstressed. The international rapid developments and population explosion all over the world have resulted in a large escalation of demand for fresh drinking water. Clean water is required for domestic, industrial, and agricultural purposes. Potable water is indispensable for life and its scarcity is growing across the world, particularly in dry regions, such as, deserts and modern industrial areas. The similar problem exists in remote areas and islands where fresh water supply through any transportation means is expensive. On the other hand, seawater exists in plenty in many parts of the world but it requires removal of salinity with additional expenses of energy which is another scarce resource. Survey reveals that approximately 79% of the available water is salty, 20% is brackish, and only 1% is fresh. Therefore, solar energy being free and abundant is being utilized in the process of desalination of brackish water to produce drinking water [1-8]. A solar still consists of a shallow basin with a transparent glass cover. The solar radiation heats the water in the basin and evaporates. The vapor begins to condense on the inner surface of the glass cover by dropwise condensation [2] and flows down into a collection trough leaving behind the salt sand impurities. Along with dropwise condensation,

*Corresponding author; e-mail: skshukla.mec@itbhu.ac.in

value of heat transfer coefficient can be 10 times larger than those associated with film condensation [9]. Extensive research work on parametric studies and methods improve the productivity of the passive solar still [6, 7]. Passive solar stills are self-operating, simple in construction, relatively free in maintenance and directly use solar energy to produce distillate water, whereas, active stills are comprised of energy concentrator to add more energy to the system for enhancing the distillate output.

A single slope basin solar still is simply an airtight rectangular shaped basin usually made of various kinds of materials. The double slope solar still has similar design to the single slope but has two glasses that sloped on two sides. It is covered with transparent material, such as, glass which is usually sloped on one side to enable condensed water to flow down to the water storage. The interior surface of the base of still is blackened to absorb solar energy to the maximum possible extent. The single slope solar still gives higher efficiency in comparison with double slope solar still in winter season [8]. However, Fath [10] found single slope solar still with a condenser in the shaded region sloped increases the still efficiency by 45%. Anil [11] used black dye injection in basin water and his result showed that a dye solution is able to increase the distillate output by 29%. Shukla and Sorayan [8] modeled the multiwick solar stills and validated the same experimentally using inner glass cover temperatures. Dev and Tiwari [12] found that a lower water depth gives better efficiency. They analyzed instantaneous gain and loss efficiency curves to give a better understanding of the performance of solar stills. Yet, the solar stills have not found commercial utility due to low productivity and the reason associated to the heat loss to the surroundings [5, 13-15]. Options like the use of energy storage system for post sunset operation has been investigated involving phase changing material (PCM) that exploited latent heat capacity to absorb the large amount of energy [16].

Abdulhaiy [13] and El-Sebaili *et al.* [14] used PCM as an energy storage medium to study the performance of stepped solar still and a single basin solar still, respectively. The productivity of solar still with PCM (SSWPCM) storage medium was found increasing during post sunset operation which occurred due to higher temperature difference between water and glass cover at relatively lower ambient temperature. El-Sebaili *et al.* [14] analyzed the transient performance of a single slope solar still with stearic acid as a storage material and observed increased productivity with increasing mass of PCM. However, they mentioned that the work on SSWPCM storage medium is still scanty.

The main objective of this work is to experimentally investigate the performance of a single slope solar still with myristic acid (99.2% purity) as PCM of various masses under simulated conditions during day in winter season using electric heater. The energy balance equations for different components of the still during charging and discharging modes have been written and solved analytically. Calculations have been carried out for daily productivity and efficiency of the still.



Figure 1. Photo of SSWOUTPCM (left) and SSWPCM (right)

Experimental procedure

A photograph and of both the single slope solar stills with and without PCM (SSWPCM and SSWOUTPCM) is given in fig. 1 whereas fig. 2 explains cross-sectional schematic side views of SSWOUTPCM and SSWPCM. The

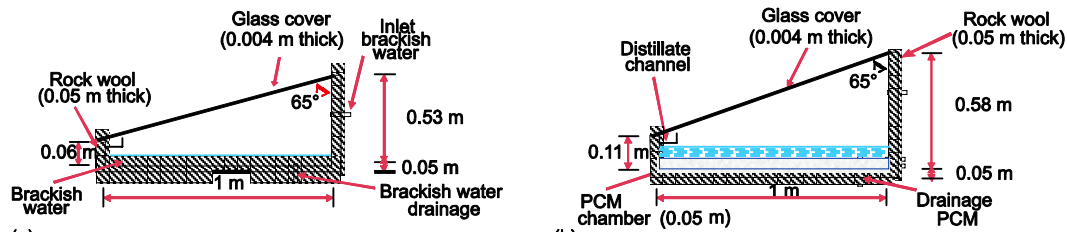


Figure 2. Cross-sectional schematic side views of (a) SSWOUTPCM, and (b) SSWPCM (for color image see journal web-site)

basin is fabricated from blackpainted 2 mm thick mild steel having an area of 1 m² each. A vertical gap beneath the horizontal portion of the basin liner is provided to upload and/or unload the PCM through a PVC pipe which takes care of the volumetric expansion of the melting PCM as well. The operational and melting temperature of PCM, in fact, governs the applicability of different types of PCM. The myristic acid relates to the class of fatty acids that have superior properties, such as, melting congruency, better chemical stability non-toxicity and better thermal reliability over many other PCM [17-20].

The measurement of PCM was done in Netzsch Technologies India Pvt Ltd, Chennai, India, by using the differential scanning calorimetry (DSC) technique. The measurements were carried out under the following conditions for the evaluation of melting and heat of fusion as shown in fig. 3: temperature range: 0-80 °C, heating rate: 10 K/min, and atmosphere: static air.

The measurements conditions of heat capacity of myristic acid are as follows as shown in fig. 4: temperature range: 0-80 °C, heating rate: 10 K/min, and atmosphere: nitrogen.

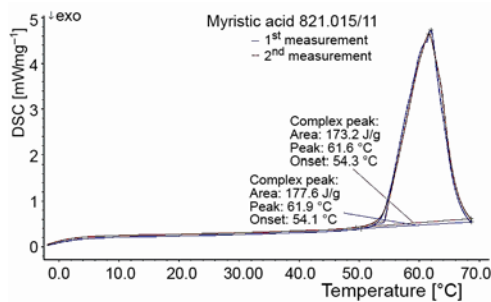


Figure 3. DSC curve for melting temperature and heat of fusion for myristic acid

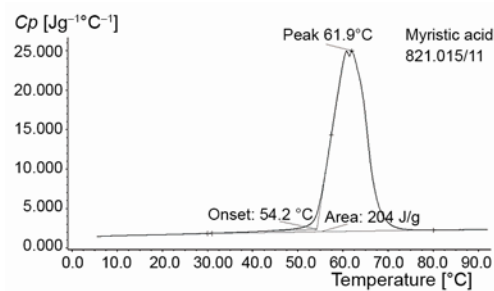


Figure 4. DSC curve for specific heat (*C_p*) of myristic acid

The measurements were repeated to check the reproducibility of the results. Therefore, myristic acid, a by-product of milk, has been used as a latent heat storage material due to its low cost and easy availability. Table 1 summarizes the thermo-physical properties of myristic acid used in the experiment [20-22].

The bottom and sides of the basin are insulated by a 5 cm thick layer of rock wool contained in an aluminum tray. The top cover of the still is made up of 4 mm thick window glass which inclines at an angle of 25° with horizontal. The condensate water is collected in a U-shaped channel fitted along the lower edge of the glass cover and carries it to the storage. Two electric heaters of 1000 W each are fixed on the basin wall for the uniform charging pur-

Table 1. Thermo-physical properties of myristic acid

Properties	Value
Meltingpoint	50-54 [°C]
Latent heat of fusion	177 [kJkg ⁻¹]
Thermal conductivity	0.25 [22] [Wm ⁻¹ °C ⁻¹]
Specific heat solid at 35 °C liquid at 55 °C	1700 [Jkg ⁻¹ °C ⁻¹] 2040 [Jkg ⁻¹ °C ⁻¹]
Density solid liquid	990 [kgm ⁻³] 861 [kgm ⁻³]

poses. Two variac transformers are employed to vary the delivered power to the systems. A temperature scanner (Altop Industries Ltd, India Sn.1005164, model ADT 5003) with resolution 0.1 °C has been used to record the temperature with *k*-type thermocouples in solar stills.

The power delivered from the heater is:

$$\text{power} = V i \cos\phi \quad (1)$$

where *V* is the voltage, *i* – the current, and $\cos\phi$ – the power factor.

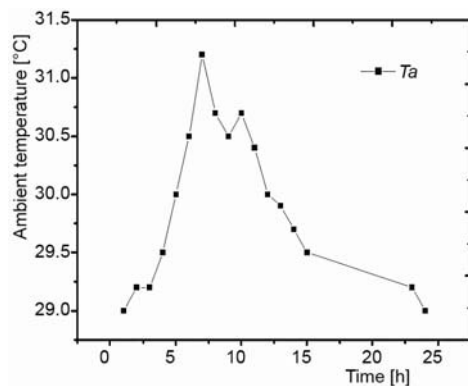
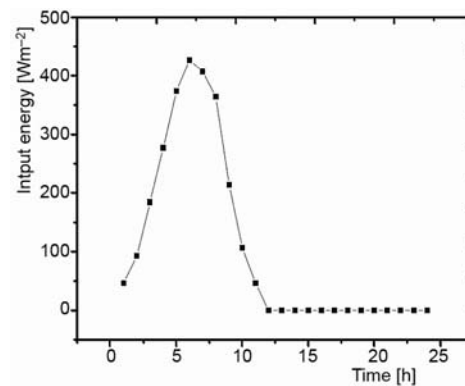
The total solar power received from the sun is represented by:

$$\text{power} = I(t)A_b \quad (2)$$

where *I*(*t*) is the solar radiation and *A_b* – the area of solar still basin, thus:

$$\text{power} = V i \cos\phi = I(t)A_b \quad (3)$$

The power input from the heater has been controlled every hour by altering voltage and current consequently. The variations of the ambient laboratory temperature and input energy have been shown in figs.5 and 6. The experimental observation has been taken from 7 a. m. (shown as 0:00 h) to 7 p. m. (shown as 12:00 h) under simulated conditions. Different water masses, *i. e.*, 30, 40, and 50 kg and PCM masses, *i. e.*, 10, 20, and 30 kg have been used. The power supply is varied from (0 to 426.2) W/m².

**Figure 5. Variation of ambient temperature to solar still for 24 hours****Figure 6. Variation of power input to solar still with variation for 24 hours**

Thermal analysis

The following assumptions have been made in order to write the energy balance equations:

- Solar still distillation unit is vapor-leakage proof.
- The conduction of heat transfer mode is between PCM and basin liner.
- The temperature gradient through PCM is negligible; it means T_{pcm} represents average temperature through the PCM chamber.

- Temperature gradients in the water are neglected.
- The heat conduction between PCM and liners is 1-D.
- The experiments are carried out under atmospheric pressure.
- Condensate is not a thermal resistance to heat flows through the glass cover, *etc.*

Passive solar still without PCM

- Energy balance for outer surface of glass cover:

$$\frac{k_g}{L_g}(T_{gin} - T_{go}) = h_2(T_{go} - T_a) \quad (4)$$

- Energy balance for inner surface of glass cover:

$$h_1(T_w - T_{gin}) = \frac{k_g}{L_g}(T_{gin} - T_{go}) \quad (5)$$

- Energy balance for water mass:

$$h_3(T_b - T_w) = m_w C_w \frac{dT_w}{dt} + h_1(T_w - T_{gin}) \quad (6)$$

- Energy balance for basin liner:

$$\alpha_b I(t) = h_3(T_b - T_w) + h_b(T_b - T_a) \quad (7)$$

From eqs. (4) and (5) can be obtained T_{go} :

$$T_{go} = \frac{\frac{k_g}{L_g} T_{gin} + h_2 T_a}{h_2 + \frac{k_g}{L_g}} \quad (8)$$

From eqs. (8) and (5) can be obtained T_{gin} :

$$T_{gin} = \frac{h_1 T_w + U_{ga} T_a}{U_{ga} + h_1} \quad (9)$$

From eq. (7) can be found T_b :

$$T_b = \frac{\alpha_b I(t) + h_2 T_w h_b T_a}{h_2 + h_b} \quad (10)$$

Finally, by substituting eqs. (9) and (10) in eq. (6), we obtain:

$$\frac{dT_w}{dt} + a T_w = f(t) \quad (11)$$

The solution of eq. (11) can be obtained using integration factor with boundary condition when $t = 0$ that $T_w = T_{wo}$ thus:

$$T_w = \frac{\overline{f(t)}}{a}(1 - e^{-at}) + T_{wo} e^{-at} \quad (12)$$

where $\overline{f(t)}$ is the average value of $f(t)$ for time interval 0 to t .

The still with the PCM charging mode

In this case eqs. (4), (5), and (6) remain same.

– Energy balance of the basin liner:

$$\alpha_b I(t) = h_3(T_b - T_w) + h_{bc}(T_b - T_{pcm}) \quad (13)$$

– Energy balance of the PCM:

$$h_{bc}(T_b - T_{pcm}) = \left(\frac{M_{equ}}{A_b} \right) \left(\frac{dT_{pcm}}{dt} \right) + h_b(T_{pcm} - T_a) \quad (14)$$

where h_b is the back loss coefficient and M_{equ} is the equivalent heat capacity of the PCM. It was expressed in [13, 14]:

$$M_{equ} = m_{pcm} C_{s,pcm} \text{ for } T_b < T_{mt}$$

$$M_{equ} = m_{pcm} L_{s,pcm} \text{ for } T_b < T_{mt} + \delta$$

$$M_{equ} = m_{pcm} C_{s,pcm} \text{ for } T_b > T_{mt}$$

Temperatures T_{go} , T_{gin} , and T_b can be obtained from eqs. (4), (5), and (13):

$$T_{go} = \frac{\frac{k_g}{L_g} T_{gin} + h_2 T_a}{h_2 + \frac{k_g}{L_g}} \quad (15)$$

$$T_{gin} = \frac{h_1 T_w + U_{ga} T_a}{U_{ga} + h_1} \quad (16)$$

$$T_b = \frac{\alpha'_b I(t) + h_2 T_w + h_{bc} T_a}{h_2 + h_{bc}} \quad (17)$$

From energy eq. (6) and introducing eqs. (16) and (17) follows::

$$\frac{dT_w}{dt} + a_c T_w = f_c(t) \quad (18)$$

With the boundary condition $t = 0, T_w = T_{wo}$ the solution of eq. (18) is:

$$T_w = \frac{\overline{f_c(t)}}{a_c} (1 - e^{-a_c t}) + T_{wo} e^{-a_c t} \quad (19)$$

and from eqs. (14) and (15) T_{pcm} can be found:

$$T_{pcm} = \frac{\overline{f_{cl}(t)}}{a_{cl}} (1 - e^{-a_{cl} t}) + T_{pcmo} e^{-a_{cl} t} \quad (20)$$

The still with the PCM discharging mode

The energy balance equation for the PCM at the interval time Δt may be written as:

$$\frac{m_{\text{pcm}} L_{\text{pcm}}}{A_b} \Delta t = h_{\text{bd}} (T_{\text{pcm}} - T_b) + h_{\text{bd}} (T_{\text{pcm}} - T_a) \quad \text{for } T_{\text{pcm}} = T_{\text{mt}} \quad (21)$$

$$h_{\text{bd}} (T_{\text{pcm}} - T_b) + h_b (T_{\text{pcm}} - T_a) = \frac{M_{\text{equ}}}{A_b} \frac{dT_{\text{pcm}}}{dt} \quad \text{for } T_{\text{pcm}} \neq T_{\text{mt}} \quad (22)$$

where $M_{\text{equ}} = m_{\text{pcm}} C_{p1,\text{pcm}}$ for $T_{\text{pcm}} > T_{\text{mt}}$, $M_{\text{equ}} = m_{\text{pcm}} C_{ps,\text{pcm}}$ for $T_{\text{pcm}} < T_{\text{mt}}$, and $h_{\text{bd}} = k_{\text{pcm}}/x_{\text{pcm}}$ that is the conductive heat transfer coefficient from the PCM to the basin liner.

The energy balance of the glass cover's inner surface and energy balance of the glass cover's outer surface remain same as expressed by eqs. (4) and (5).

– Energy balance of the water mass:

$$h_3 (T_b - T_w) = m_w \frac{Cp_w}{A_b} \frac{dT_w}{dt} + h_1 (T_w - T_{\text{gin}}) \quad (23)$$

– Energy balance of the basin liner:

$$h_3 (T_b - T_w) = h_{\text{bd}} (T_{\text{pcm}} - T_b) \quad (24)$$

The expressions for T_{go} and T_{gin} have been given by eqs. (15) and (16), however:

$$T_b = \frac{h_3 T_w + h_{\text{bd}} T_{\text{pcm}}}{h_3 + h_{\text{bd}}} \quad (25)$$

$$\frac{dT_w}{dt} + a_d T_w = f_d(t) \quad (26)$$

From eq. (26), using the boundary condition, $t = 0$ and $T_w = T_{w0}$ follows:

$$T_w = \frac{\overline{f(t)}}{a_d} (1 - e^{-a_d t}) + T_{w0} e^{-a_d t} \quad (27)$$

By placing T_b (eq. 25) in eq. (22), T_{pcm} was obtained:

$$T_{\text{pcm}} = \frac{\overline{f_d(t)}}{a_{d1}} (1 - e^{-a_{d1} t}) + T_{\text{pcm}0} e^{-a_{d1} t} \quad (28)$$

The productivity and efficiency of the solar still

The hourly and daily productivity of solar still is:

$$mew_h = \frac{h_{\text{ew}} (T_w - T_{\text{gin}})}{\gamma} \quad (29)$$

$$mew_d = \sum_{24 \text{ h}} mew_h$$

The instantaneous efficiency of the solar still is:

$$\eta_i = \frac{h_{\text{ew}} (T_w - T_{\text{gin}})}{I(t)} 100\% \quad (30)$$

Numerical computation

The variation of the evaporative heat transfer coefficient with temperature is highly nonlinear [23]. The non-linearity in radiation energy and water diffusion terms makes the equations difficult to solve explicitly. An iteration method is used to obtain the final solution

Table 2. Design parameters of solar still with and without PCM

Parameter	Values, units	Parameter	Values, units
A_b	1 [m ²]	R_w	0.05
A_g	1.1 [m ²]	ϵ_g	0.95
α_b	0.95	ϵ_w	0.95
α_g	0.05	m_w	30-50 [kg]
α_w	0.05	m_{pcm}	10-30 [kg]
R_g	0.05	L_{ins}	0.05 [m]
h_2	5.7+ 3.8 v [W m ⁻¹ °C ⁻¹]	L_b	0.002 [m]
K_g	0.035 [W m ⁻² °C ⁻¹]	K_b	43 [W m ⁻² °C ⁻¹]
L_g	0.004 [m]		

program to calculate the productivity of solar still with and without PCM. The program executed by using parameter design of solar still with and without PCM are shown in tab. 2.

Results and discussion

The experimental set-up was designed and installed at Renewable Energy Laboratory, Department of Mechanical Engineering, BHU, Varanasi (25°19'60 N and 83°0'0 E), India. The experiments were started at 7:00 a.m. under simulated conditions with an aim to record the temperatures of ambience, outer and inner surfaces of glass cover, basin liner, stored water and PCM at every one hour interval till 7:00 p. m. The values of operating voltage, current, and distillate output were also recorded. Table 3 (Appendix B) shows the typical values of the data recorded for 40 kg water of SS and SSWPCM on 17-10-2010 under simulated conditions. Figures 7 and 8 show the temperature variations of basin water, outer and inner surfaces of glass cover, basin liner, stored water with the time of the day. It is clear from the figures that the increase in temperature is directly proportional to the input energy which is similar to the trends of solar radiation till 6:00 p. m. The heaters are switched off at 6:00 p. m. to simulate the post sunset condition. The latent energy stored in the myristic acid keeps the system operational during the night to deliver distillate output. However, the decreasing trend of all above temperatures show that the quantity of distillate output is reduced, figs. 9(a) and 9(b) due to little difference in the temperature of glass cover and ambience that continues until next day morning.

Further, the productivity for given mass of water in the basin of the SSWPCM has been plotted for daytime and night hours separately to understand the operational characteris-

[24]. The classical method of optimization has been used to solve the problem. On the other hand, if the optimization involves the objective function that is not stated as explicit function of the design variables, we cannot solve it by using the classical analytical method. In such case we need to use the numerical method of optimization for solution. For this purpose Newton Raphson method has been chosen [25]. The iteration process starts with a guess for all values of dependent variables [26]. Two programs of 'C' language have been developed to find the predicted theoretical values from eqs. (4)-(29), first one isto calculate parameters 'c' and 'n' for eq. (A-2) appendix A, with the help of T_w and T_{gin} observed data. These value have been used with the second developed

tics of the system. Figure 9(a) shows that the productivity decreases with the increase of the mass of water during daytime, and it is due to the fact that higher quantity of water needs relatively more energy to raise its temperature before being evaporated. However, the productivity increases with the increasing water mass during night hours, fig. 9(b) due to relatively larger storage of energy in PCM as latent and sensible heat in higher water mass. It was also observed that no significant increase in productivity was found when quantity was increased beyond 20 kg. The productivity of the SSWOUTPCM and SSWPCM is shown in fig. 10. It is observed that the PCM enhances the productivity of the system by 35-40 % due to PCM's being as heat as source under discharge mode during night.

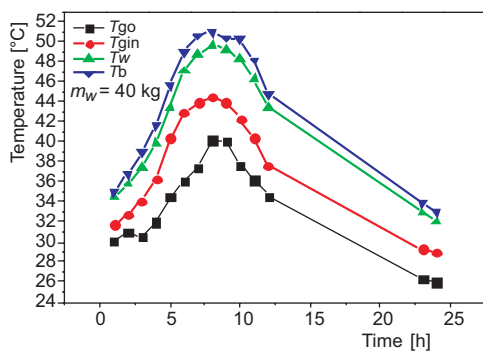


Figure 7. Variation of temperatures of the SSWOUTPCM during the day (for color image see journal web-site)

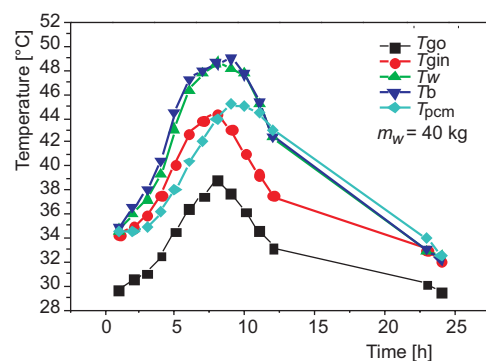


Figure 8. Variation of temperature of the SSWPCM during the day (for color image see journal web-site)

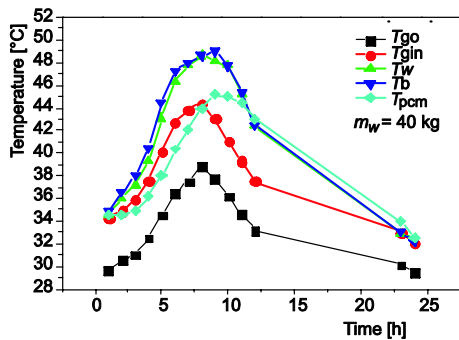


Figure 9(a). Variation of daytime productivity from solar still with and without PCM for $m_w = 50$ kg (for color image see journal web-site)

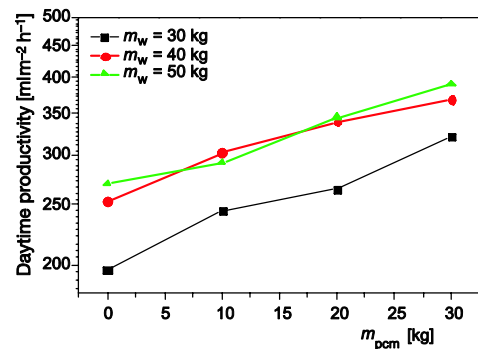


Figure 9(b). Variation of night productivity from solar still with and without PCM (for color image see journal web-site)

The variation of total distillate output of different water masses has been plotted for 24 hours duration, fig. 11. The decreasing trend of the curve in fig. 11 indicates that the thicker water depth in solar still basin yields lower distillate output over 24 hours, and the reason relates to the conversion of major portion of energy to sensible heat due to higher heating capacity of water mass. Further the solar still with 20 kg of PCM provides more daily productivity than 30 kg of PCM. This is due to the reason that if the mass of PCM increases, the rate of melting decreases and heat doesn't reach every part of the chamber, therefore, phase change doesn't take place everywhere in the PCM chamber. From fig. 2, it can be seen that Rockwool

insulation is provided in the bottom and sides of the basin to reduce any heat transfer from solar still to the environment through PCM. However during experimentation, for better estimation of output, insulation temperature was also measured to quantify the losses from solar stills. This study reveals that the difference in the temperature between insulator and ambience is more significant in the still without PCM than the solar still with PCM, fig. 12. The daily productivity of PCM (30 kg) with three different water masses has been shown in fig. 13. It is observed that the overall productivity does not change significantly for 24 hours, but the day and night hours' productivities differ significantly, figs. (7) and (8). Though the higher mass of PCM enhances the productivity during night hours, the quantum of the output is yet lower than that obtained during day hours. Therefore, the higher mass of PCM could not contribute significantly to the distillate output.

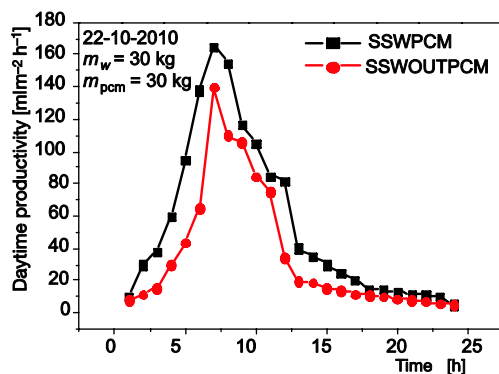


Figure 10. Variation of daily productivity of the SSWPCM and SSWOUTPCM during the day

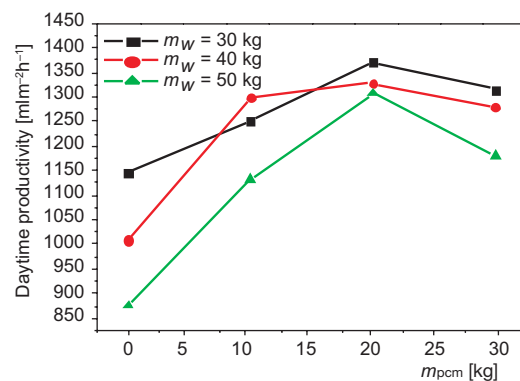


Figure 11. Variation of total distillate output of different water masses

(for color image see journal web-site)

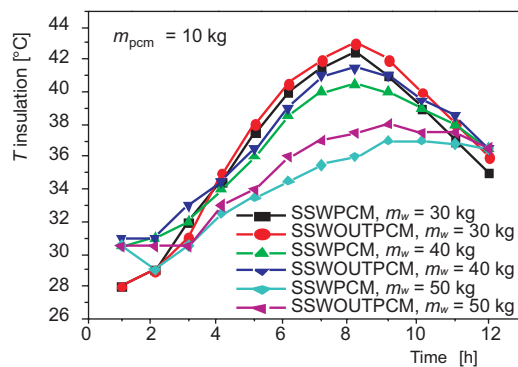


Figure 12. Variation of insulation temperature of the solar still with and without PCM for all water mass at $m_{pcm} = 10$ kg

(for color image see journal web-site)

observed data and deviation falls within $\pm 28\%$ for SSWOUTPCM and $\pm 31\%$, 31% and 20% for SSWPCM with PCM mass of 10 kg and water masses of 30, 40 and 50 kg, respectively.

The increased/decreased deviation, *i. e.*, 28%, 31%, 23% for 20 kg PCM, 21%, 27%, 23% for 30 kg of PCM is reported between predicted and observed data. The variation of the

In order to note the effect of outdoor environment on the productivity, the similar data of solar still without PCM with 40 kg mass of water in outdoor environments [27] is compared with simulated results obtained from this study as shown in fig. 14. The similar trend has been noted with some difference in the productivity, which may be attributed to the difference in the climatic conditions of Varanasi and Delhi. Further, the energy balance equations, eqs. (4)-(35) were applied to predict the distillate output from solar stills, with and without PCM, for the comparison with the observed data. It is inferred from figs. (15) and (16) that there is reasonable agreement between the theoretical and observed

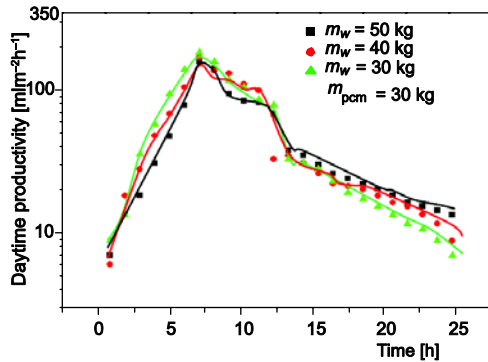


Figure 13. Variation of hourly productivity due to SSWPCM
 (for color image see journal web-site)

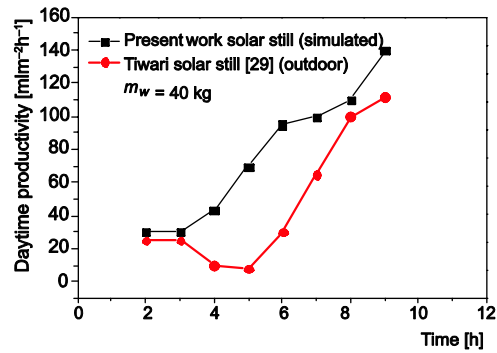


Figure 14. Daily productivity for different type of solar still at same power supply when $m_w = 40$ kg

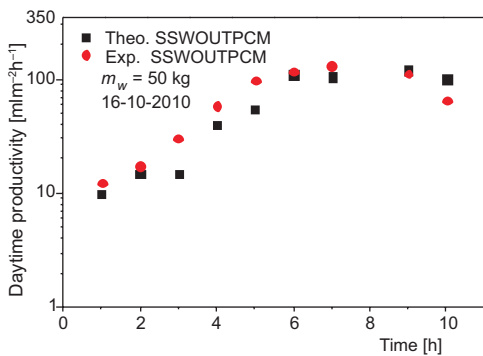


Figure 15. Comparison of predicted and observed production for SSWOUTPCM

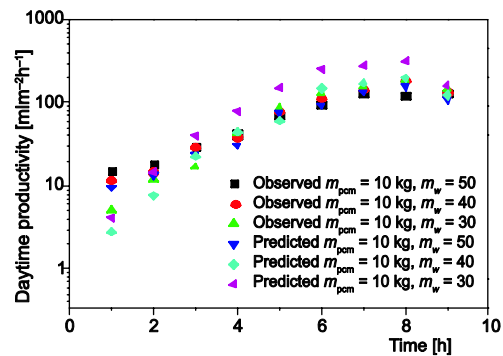


Figure 16. Comparison of predicted and observed production for SSWPCM of $m_{pcm} = 10$ kg
 (for color image see journal web-site)

instantaneous efficiency of the solar stills with and without PCM has been plotted in fig. 17. It is observed that the instantaneous efficiency of the SSWPCM is always higher than the traditional still. However, the increasing trend of both the curves with time indicates that the instantaneous efficiency keeps increasing due to increased temperature difference between basin water and ambience.

Conclusions

Thermal energy storage is known as one of the best solutions for tackling cooling and heating issues in narrow temperature range, as well as one of the most environmentally friendly technologies. This study shows the potential of integration of phase change material with solar still system for producing potable water

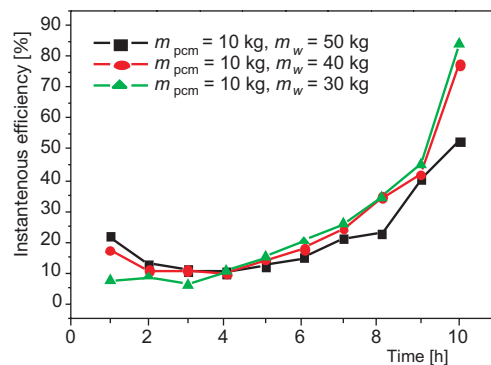


Figure 17. Variation of instantaneous efficiency for SSWPCM when $m_{pcm} = 10$ kg
 (for color image see journal web-site)

in rural, semi urban and urban areas throughout the day and night. The preliminary results show that the system dramatically increases the productivity of 35-40% as compared to conventional solar stills. Further it was found that the highest productivity rate varied with the least water depth in the basin of solar still system. It is also noted that for this particular shape and size of the distillation system for getting higher heat transfer, which in turn gives highest productivity, 20 kg mass of PCM (*i. e.* myristic acid) should be loaded in the chamber. It is also inferred that there is a reasonable agreement between experimental and predicted results by considering inner glass cover temperature, which is in accordance with the results of previous researchers [3,8].

Nomenclature

A	– area, [m ²]	U_i	– top loss coefficient, [Wm ⁻²]
C_p	– specific heat, [Jkg ⁻¹ °C ⁻¹]	U_L	– overall heat transfer coefficient, [Wm ⁻²]
dt	– time interval, [s]	V	– voltage, [volt]
Gr	– Grashof number, [-]	v	– wind speed, [ms ⁻¹]
h	– heat transfer coefficient, [Wm ² °C ⁻¹]	Greek symbols	
h_b	– back loss coefficient, [Wm ² °C ⁻¹]	α	– absorptivity, [-]
h_{bc}	– conductive heat transfer coefficient from basin liner to PCM, [Wm ² °C ⁻¹]	α'	– fraction of solar energy absorbed, [-]
h_{bd}	– conductive heat transfer coefficient from the PCM to the basin liner, [Wm ² °C ⁻¹]	γ	– latent heat of vaporization, [Jkg ⁻¹]
h_{cw}	– convective heat transfer coefficient from water surface to the glass cover, [Wm ² °C ⁻¹]	δ	– incremental rise, [°C]
h_{ew}	– evaporative heat transfer coefficient from water surface to the glass cover, [Wm ² °C ⁻¹]	ε	– emissivity, [-]
h_{rw}	– radiative heat transfer coefficient from water surface to the glass cover, [Wm ² °C ⁻¹]	η_i	– instantaneous efficiency, [%]
h_1	– total heat transfer coefficient from water to glass cover, [Wm ² °C ⁻¹]	τ	– transmittance coefficient
h_2	– convective heat transfer coefficient from glass to ambient, [Wm ² °C ⁻¹]	σ	– Stefan-Boltzmann constant, (= 5.6697·10 ⁻⁸), [Wm ⁻² °C ⁻⁴]
h_3	– convective heat transfer coefficient from basin liner to water, [Wm ² °C ⁻¹]	Subscripts	
i	– current, [A]	a	– ambient
$I(t)$	– solar flux on an inclined collector, [Wm ⁻²]	b	– basin, back
K	– thermal conductivity, [Wm°C ⁻¹]	c	– convective
L, x	– thickness, [m]	d	– day
L	– latent heat of fusion, [Jkg ⁻¹]	e	– evaporative
m	– mass, [kg]	eff	– effective
mew	– productivity of distillate water, [mlm ⁻² h ⁻¹]	f	– film temperature
P	– partial pressure, [N/m ²]	g	– glass
Pr	– Prandtl number, [-]	gin	– inner glass
Ra	– Rayleigh number, [-]	go	– outer glass
T	– temperature, [°C]	h	– hour
T_{wo}	– water temperatures at time zero, [°C]	ins	– insulation
T_{pcmo}	– temperature of phase change material at time zero, [°C]	l	– liquid
ΔT	– effective temperature difference [°C]	mt	– melting
U_b	– overall bottom loss coefficient, [Wm ⁻²]	pcm	– phase change material
U_{bd}	– overall heat transfer coefficient from PCM to the basin liner, [Wm ⁻¹]	r	– radiation
U_{ga}	– overall heat transfer coefficient from inner glass to ambient, [Wm ⁻²]	s	– solid
		w	– water
		Acronyms	
		PCM	– phase change material
		SSWPCM	– solar still with phase change material
		SSWOUTPCM	– solar still without phase change material

Appendix A

The details of parameters in equations are described:

$$h_1 = h_{cw} + h_{ew} + h_{rw} \quad (\text{A-1})$$

$$h_{cw} = C \frac{k_f}{d} \text{Ra}_f^n \quad (\text{A-2})$$

$$\text{Ra}_f = \text{Gr}_f \text{Pr}_f, \quad \text{Gr}_f = \frac{d^3 \rho_f^2 \beta \Delta T'}{\mu_f^2}, \quad \text{Pr}_f = \frac{\mu_f C_f}{K_f} \quad (\text{A-3})$$

$$\Delta T' = \left[(T_w - T_{gin}) + \frac{(P_w - P_g)(T_w + 273.15)}{26800 - P_w} \right] \quad (\text{A-4})$$

$$P_w = e^{\left(25.317 - \frac{5144}{T_w + 273.15} \right)} \quad (\text{A-5})$$

$$P_{gin} = e^{\left(25.317 - \frac{5144}{T_{gin} + 273.15} \right)} \quad (\text{A-6})$$

$$h_{ew} = 16.273 \cdot 10^{-3} \left[\frac{h_{cw}(P_w - P_g)}{T_w - T_{gin}} \right] \quad (\text{A-7})$$

$$h_{rw} = \varepsilon_{\text{eff}} \sigma \left[(T_w + 273.15)^2 + (T_{gin} + 273.15)^2 \right] (T_w - T_{gin} + 546), \quad \varepsilon_{\text{eff}} = \left(\frac{1}{\varepsilon_w} + \frac{1}{\varepsilon_g} - 1 \right)^{-1} \quad (\text{A-8})$$

$$h_2 = h_{ca} + h_{ra} = 5.7 + 3.8 v \quad (\text{A-9})$$

where $v = 2$ m/s.

$$h_3 = 0.54 \frac{k_w}{x_c} \text{Ra}_f^{1/4}, \quad \text{Ra}_f < 8 \cdot 10^6 \quad (\text{A-10})$$

$$h_3 = 0.15 \frac{k_w}{x_c} \text{Ra}_f^{1/3}, \quad \text{Ra}_f > 8 \cdot 10^6 \quad (\text{A-11})$$

$$h_b = \left(\frac{L_{\text{ins}}}{K_{\text{ins}}} + \frac{1}{h_i} \right)^{-1} \quad (\text{A-12})$$

$$f(t) = \frac{\alpha_{\text{eff}} I(t) + T_a U_L}{m_w C_w} \quad (\text{A-13})$$

$$a = \frac{U_L}{m_w C_w} \quad (\text{A-14})$$

where

$$U_L = U_t + U_b, \quad U_t = \frac{h_1 U_{ga}}{h_1 + U_{ga}}, \quad U_b = \frac{h_3 h_b}{h_3 + h_b}, \quad \alpha_{\text{eff}} = U_1 \alpha_b,$$

$$U_1 = \frac{h_3}{h_3 + h_b}, \quad U_2 = \frac{h_1}{h_1 + U_{ga}}, \quad U_{ga} = \frac{\frac{K_g}{L_g} h_2}{\frac{K_g}{L_g} h_2}$$

$$fc(t) = \frac{a_{\text{eff}} I(t) + U_b T_{\text{pcm}} + U_t T_a}{m_w C_w} \quad (\text{A-15})$$

$$a_c = \frac{U_{Lc}}{m_w C_w} \quad (\text{A-16})$$

where

$$U_{Lc} = U_t + U_{bc}, \quad U_{bc} = \frac{h_3 h_{bc}}{h_3 + h_{bc}}, \quad \alpha_{\text{effc}} = U_{1c} \alpha_b, \quad U_{1c} = \frac{h_3}{h_3 + h_{bc}}$$

$$fc1(t) = \frac{\alpha_b I(t) U_3 + h_b T_a + U_{bc} T_w}{m_{\text{equ}}} \quad (\text{A-17})$$

$$a_{c1} = \frac{U_L + h_b}{m_{\text{equ}}} \quad (\text{A-18})$$

where $U_3 = \frac{h_{bc}}{h_3 + h_{bc}}$

$$fd(t) = \frac{U_{bd} T_{\text{pcm}} + U_t T_a}{m_w C_w} \quad (\text{A-19})$$

$$a_d = \frac{U_{Ld}}{m_w C_w} \quad (\text{A-20})$$

$$fd1(t) = \frac{-U_{bd} T_w - h_b T_a}{m_{\text{equ}}} \quad (\text{A-21})$$

$$ad1 = \frac{U_{bd} + h_b}{m_{\text{equ}}} \quad (\text{A-22})$$

where $U_{Ld} = U_t + U_{bd}$, $U_{bd} = \frac{h_3 h_{bd}}{h_3 + h_{bd}}$

Appendix B

Table 3. Experimental data of SSWOUTPCM and SSWPCM on 17-10-2010

SSWPCM									SSWOUTPCM				
Time [h]	Power [W m ⁻²]	T _a [°C]	T _{go} [°C]	T _{gin} [°C]	T _w [°C]	T _b [°C]	T _{pcm} [°C]	Output [ml]	T _{go} [°C]	T _{gin} [°C]	T _w [°C]	T _b [°C]	Output [ml]
7-8	46.2	30.1	29.6	34.3	34.6	35.1	39.4	4	30.1	31.7	34.5	35	2
8-9	92.8	30.8	30.6	34.9	36	37	39.6	40	30.9	32.8	35.8	36.8	30
9-10	184.3	31.2	31	35.9	37.2	38.7	40	37	30.5	34.1	37.5	39	30
10-11	276.6	31.5	32.5	37.6	39.3	41.1	41.4	65	32	36.3	39.9	41.7	43
11-12	374.0	31.4	34.5	40.1	43.1	45.2	43.5	80	34.5	40.4	43.5	45.7	70
12-13	426.2	31.8	36.5	42.7	46.3	48	45.6	110	36	49.8	47.1	49	95
13-14	406.9	31.7	37.5	43.9	47.7	49.7	47.5	140	37.5	44	48.8	50.6	100
14-15	364.2	31.2	38.9	44.4	48.6	50.2	49.3	180	40.2	44.5	49.7	51	140
15-16	213.0	29.8	37.8	43.1	48.2	49.7	50.4	150	40.1	44	49.2	50.4	110
16-17	106.6	30	36.2	41	47.7	49.5	50	90	37.7	42.3	48.4	50.3	105
17-18	46.2	30.4	34.6	39.3	45.2	47.1	48.6	87	36.2	40.4	46.3	48.2	75
18-19	0	30.2	33.2	37.5	42.4	43.8	47.5	85	34.6	37.6	43.4	44.8	70
6:00	0	30.7	30.1	34.9	32.9	33.9	37.9	250	26.3	29.3	32.9	33.9	185
7:00	0	30.7	29.5	34.1	35.3	36	39.6	10	30.3	31.6	35.3	36	5

References

- [1] Bachir, B., A Solar Desalination Plant for Domestic Water Needs in Arid Areas of South Algeria, *Desalination*, 153 (2003), 1-3, pp. 65-69
- [2] Taiwo, M. O., Improving the Performance of Solar Stills Using Sun Tracking in Mechanical Engineering, M. Sc. thesis, Faculty of Engineering, University of Strathclyde, Glasgow, Scotland, 2010
- [3] Shukla, S. K., Rai, A. K., Analytical Thermal Modelling of Double Slope Solar Still by Using Inner Glass Cover Temperature, *Thermal Science*, 12 (2008), 3, pp. 139-152
- [4] Shukla, S. K., Product Cost Calculations of Various Designs of Conventional Solar Still Systems, *Int. Journal of Agile Systems and Mgmt.*, 4 (2009), 1/2, pp. 86-97
- [5] Akash, B. A., et al., Experimental Evaluation of a Single-Basin Solar Still Using Different Absorbing Materials, *Renewable Energy*, 14 (1998), 1-4, pp. 307-310
- [6] Nafey, A. S., et al., Parameters Affecting Solar Still Productivity, *Energy Conversion and Management*, 41 (2000), 16, pp. 1797-1809
- [7] Badran, O. O., Experimental Study of the Enhancement Parameters on a Single Slope Solar Still Productivity, *Desalination*, 209 (2007), 1-3, pp. 136-143
- [8] Shukla, S. K., Sorayan, V. P. S., Thermal Modeling of Solar Stills: An Experimental Validation: Renewable Energy, *Fuel and Energy Abstracts*, 30 (2005), 5, pp. 683-699
- [9] Cengel, Y. A., *Heat and Mass Transfer – A practical Approach*, 3rd ed., Tata McGraw-Hill Publishing Company Limited, New Delhi, India, 2007
- [10] Fath, H., Solar Distillation: a Promising Alternative for Water Provision with Free Energy, a Simple Technology and a Clean Environment, *Desalination*, 116 (1998), 1, pp. 45-56
- [11] Anil, K. R., Effect of Various Dyes on Solar Distillation, *Solar Energy*, 27 (1981), 1, pp. 51-65

- [12] Dey, R., Tiwari, G. N., Characteristic Equation of a Passive Solar Still, *Desalination*, 245 (2009), 1-3, pp. 246-265
- [13] Abdulhaiy, M. R., Transient Analysis of a Stepped Solar Still for Heating and Humidifying Greenhouses, *Desalination*, 161 (2004), 1, pp. 89-97
- [14] El-Sebaei, A. A., *et al.*, Thermal Performance of a Single Basin Solar Still with PCM as a Storage Medium, *Applied Energy*, 86 (2009), 7-8, pp. 1187-1195
- [15] Nafey, A. S., *et al.*, Enhancement of Solar Still Productivity Using Floating Perforated Black Plate, *Energy Conversion and Management*, 43 (2002), 7, pp. 937-946
- [16] Agyenim, F., *et al.*, A Review of Materials, Heat Transfer and Phase Change Problem Formulation for Latent Heat Thermal Energy Storage Systems (LHTESS), *Renewable and Sustainable Energy Reviews*, 14 (2010), 2, pp. 615-628
- [17] Kaygusuz, K., Sari, A., Renewable Energy Potential and Utilization in Turkey, *Energy Conversion and Management*, 44 (2003), 3, pp. 459-478
- [18] Sari, A., Kaygusuz, K., Some Fatty Acids Used for Latent Heat Storage Thermal Stability and Corrosion of Metals with Respect to Thermal Cycling, *Renewable Energy*, 28 (2003), 8, pp. 939-948
- [19] Sari, S., Thermal Reliability Test of Some Fatty Acids as PCMs Used for Solar Thermal Latent Heat Storage Applications, *Energy Conversion and Management*, 44 (2003), 14, pp. 2277-2287
- [20] Sari, A., Kaygusuz, K., Thermal Performance of Myristic Acid as a Phase Change Material for Energy Storage Application, *Renewable Energy*, 24 (2001), 2, pp. 303-317
- [21] Sharma, D., *et al.*, Phase Change Materials for Low Temperature Solar Thermal Applications, *Res. Rep. Fac. Eng. Mie Univ.*, 29 (2004), 1, pp. 31-64
- [22] Buddhi, D., *et al.*, A Simplification of the Differential Thermal Analysis Method to Determine the Latent Heat of Fusion of Phase Change Materials, *J. Phys. D: Appl. Phys.*, 20 (1987), 3, pp. 1601
- [23] Sharma, V.B., Mullick, S.C., Estimation of Heat-Transfer Coefficients, the Upward Heat Flow, and Evaporation in a Solar Still, *Journal of Solar Energy Engineering*, 113 (1991), 1, pp. 36-41
- [24] Yung, C. S., Lansing, F. L., *Performance Simulation of the JPL Solar-Powered Distiller, Part 1: Quasi-Steady-State Conditions*, The Telecommunications and Data Acquisition Progress Report, pp. 142-160, 1982
- [25] Rao, S. S., *Engineering Optimization Theory and Practice*, 3rd enlarged ed., New Age international Publishers, New Delhi, India, 2010
- [26] Majumdar, P., *Computational Methods for Heat and Mass Transfer*, Taylor and Francis, New York, USA, 2005
- [27] Tiwari, A. K., *Annual Performance of Solar Stills for Different Inclinations of Condensing Covers and Water Depths*, Ph. D. thesis, Indian Institute of Technology, New Delhi, India, 2006